Synthesis of Activated Carbon from Dragon Fruit Peel for Adsorption of Methyl Blue

Thi Ngoc Diem Tran[1], Thi Tuu Tran[2,3], Bich Ngoc Hoang[2,3], Van Tan Lam[2,3], and Thi Cam Quyen Ngo[2,3*]

[1]*Faculty of Chemical Engineering and Food Technology, Nong Lam University, Quarter 6, Linh Trung Ward, Thu Duc City, Ho Chi Minh 700000, Vietnam*

[2]*Faculty of Food and Environmental Engineering, Nguyen Tat Thanh University, 300A Nguyen Tat Thanh Street, Ward 13, District 4, Ho Chi Minh 700000, Vietnam*

[3]*Institute of Applied Technology and Sustainable Development, Nguyen Tat Thanh University, No. 1 Vo Chi Cong Street, Long Thanh My Ward, Thu Duc City, Ho Chi Minh 700000, Vietnam*

** **Corresponding author:***

tel: +84-964240067
email: ntcquyen@ntt.edu.vn

Received: June 7, 2023
Accepted: June 4, 2024

DOI: 10.22146/ijc.85429

Abstract: *In this study, activated carbon from dragon fruit peel was synthesized and applied for its ability to adsorb organic pigments in water. The results obtained from the SEM and FTIR analyzes revealed the presence of the characteristic functional groups of activated carbon. The adsorption capacity of synthetic activated carbon was evaluated against methylene blue dye. This study also evaluated factors affecting the adsorption process, including time, content, temperature, concentration, and solution pH. The optimal adsorption conditions were recorded at pH 6, concentration 95 mg/L, time 43 min, and temperature 30 °C. At optimal adsorption conditions, the adsorption capacity predicted from the model is said to be 54.12 mg/g with an efficiency of 27.5%. The experimental data of the study were evaluated using adsorption kinetic models and adsorption isotherm models of the material. The results showed that the activated carbon material from dragon fruit peel is a potential material in the application for adsorbing pollutant dyes in wastewater.*

Keywords: *adsorption; methylene blue; dragon fruit peel; adsorption kinetic model; adsorption isotherm model*

■ INTRODUCTION

Today, the development of industries and people's quality of life are increasingly improved. However, it comes with pollution to the land, air and especially water environment. The primary industry causing water pollution is the textile industry. The composition of textile dyeing wastewater contains many compounds that are difficult to biodegrade, high concentration, and many organic substances with biological toxicity, such as carcinogenic [1], congenital disabilities, and mutagenic [2]. Therefore, it is necessary to have a method of treating wastewater before it is discharged.

The treatment methods used for many years can be broadly classified as treatment methods, such as electrochemical [3], oxidation [4-5], flocculation-make cotton [6], membrane [7], and adsorption [8-10]. Among these techniques, adsorption remains an effective method to remove contaminants due to advantages such as lower cost, higher adsorption capacity, and environmental friendliness [10]. Activated carbon can be produced from plant materials, very carbon-rich organic materials, or petrochemicals. Agricultural by-products are an abundant source of raw materials to produce activated carbon.

Vietnam is currently the country with the largest area and output of dragon fruit in Asia. Binh Thuan is the capital of dragon fruit with an area of over 22,000 ha, with a total output of about 400,000 tons. Dragon fruit is processed into many different products, such as dried dragon fruit, juice, wine, candy, and syrup, mostly for domestic consumption with a processing capacity of

about 182,000 tons/year. On the other hand, the discarded dragon fruit peel after processing will be an abundant source of raw materials to produce activated carbon, helping to bring economic value and reduce the problem of environmental pollution. To take advantage of raw materials from by-products, the project "research on synthesizing activated carbon from dragon fruit peel using organic colorants treatment" was carried out by the research team.

Activated carbon has long been known as an effective adsorbent for organic pigments in industrial wastewater. In recent years, scientists have studied the synthesis of activated carbon from agricultural by-products, optimizing adsorption conditions to solve the problem of environmental pollution. Ahmad et al. [11] conducted a study on synthesizing activated carbon made from passion fruit peel to treat methylene blue. Lu et al. [12] synthesized activated carbon from dragon fruit peel. Jawad et al. [13] have studied the synthesis of activated carbon from dragon fruit peel, activated by KOH to adsorb methylene blue. Ahmad et al. [14] conducted a study on synthesizing activated carbon from dragon fruit peels to remove methylene blue in water systems. Georgin et al. [15] studied the synthesis of activated carbon from watermelon rind through microwave-assisted K_2CO_3 activation and its application to remove methylene blue dye. Neme et al. [16] studied synthesizing activated carbon from castor bean shells through H_3PO_4 impregnation and heat treatment. Purnaningtyas et al. [17] prepared activated carbon-chitosan-alginate beads powder as an adsorbent for methylene blue and methyl violet 2B. The study revealed that the carbon-chitosan-alginate beads powder gave maximum adsorption capacities of 1.34 and 1.23 mmol/g for methylene blue and methylene violet 2B. The adsorption kinetics and isotherms of dyes on the carbon-chitosan-alginate beads powder conformed to the pseudo-second-order kinetics model and Freundlich isotherm.

In this study, we used the microwave-assisted method to synthesize activated carbon from dragon fruit peel. This synthesis method helps activated carbon after synthesis to have an increased material surface area and increased pore size, which is suitable for materials used in the adsorption of organic dyes.

■ EXPERIMENTAL SECTION

Materials

Dragon fruit peel by-products collected from processing factories in Ho Chi Minh City, Vietnam. NaOH (> 99%), HCl (99%), and ciprofloxacin were purchased from Sigma-Aldrich. Crystal violet (CV), brilliant green (BG), methylene blue (MB), methyl red (MR), Congo red (CR), methyl orange (MO), and acid yellow (AY) were purchased from Sigma-Aldrich.

Instrumentation

The equipment used in this research were pH meter (HANNA HI2211 phCPR meter), magnetic stirrer, and shaker (JEIO TECH IST–4075). Characterization of the functional groups of the activated carbon was detected by Fourier transform infrared spectroscopy (FTIR–6600 type A) at 400–4000 cm^{-1} wavelength. The morphology of the activated carbon was characterized by scanning electron microscopy (SEM Hitachi S–4800). The concentration of dyes was analyzed by UV-vis spectrophotometer (Metash V-5100 Visible Spectrophoto).

Procedure

Process of synthesizing activated carbon material from dragon fruit peel

The dragon fruit peel was thoroughly washed with distilled water to eliminate impurities and dirt. Afterward, it was dried at 80 °C until a consistent weight was achieved. The dried peel was then ground into a fine powder and soaked in a NaOH solution for 24 h at 100 °C. Following this, the mixture was microwaved at 800 W for 2 min. All the chemicals and reagents used in this study were of analytical grade. The initial pH of the solution was adjusted by adding HCl and NaOH solutions.

Adsorption experiment

The effects of factors affecting the adsorption process were evaluated at different pH (2–10), initial concentration (20–100 mg/L), adsorbent content (0.5–2 g/L), and adsorption time (5–80 min). The adsorption

capacity was calculated according to the following Eq. (1).

$$q_e = \frac{C_0 - C_f}{W} \times V = \frac{C_0 - C_f}{dosC} \quad (1)$$

In this context, q_e (mg/g) denotes the adsorption capacity, while C_0 and C_f (mg/L) indicate the concentrations before and after the adsorption process, respectively. The dos C (g/L) signifies the content of the adsorbent, and W (g) represents the mass of the adsorbent used.

■ RESULTS AND DISCUSSION

Structural Properties of Materials

Material surface morphology analysis

The surface morphology of activated carbon material is shown in Fig. 1. A SEM image was adopted to examine the morphological structure of activated carbon from dragon fruit peels. Fig. 1 shows the surface morphology of activated carbon at 10 and 50 μm from dragon fruit peel synthesized by microwave method with high porosity and uneven pore size, favorable for the adsorption of organic dyes. The surface area and pore volume for small pores were evaluated using the BET method.

Analysis of the pore surface of materials – BET

The activated carbon that has been synthesized by the microwave method shows the formation of dense pores in a honeycomb shape. After analysis by the BET method, activated carbon from dragon fruit peel recorded a surface area value of 688.808 m^2/g and a pore volume of 0.0158 cm^3/g. The use of microwave support for the synthesis process has contributed to improving the surface of the material, creating more pores of small sizes. This has been proven in the study by Nayak et al. [18]. Table 1 shows that the activated carbon material from dragon fruit peel using the microwave-assisted method has nearly equivalent surface area values compared with conventional methods in the activation time and low temperature.

FTIR and XRD analysis

FTIR and XRD images of activated carbon from dragon fruit peel are shown in Fig. 2. In Fig. 2(a), the FTIR spectrum shows the fluctuation of functional groups. The O–H group is recorded in the region of displacement from the peak of 3375 cm^{-1}, the C≡C group was recorded at 2205 cm^{-1}. The peaks of 1555, 1437, 1080–1253, and 870 cm^{-1} can be assigned to vibrations of groups C=C (aromatic), C–H (methyl, alkane), C–O (ester, ether, phenol), and C–H (aromatic hydrogen) [19-20]. The functional groups are also similar in the study of Jawad et al. [13] and Ahmad et al. [14]. The XRD spectrum of activated carbon is shown in Fig. 2(b). The diffraction peaks at 2θ = 29.8 and 40° show the characteristic structure. The 29.8° peak indicates the presence of graphite crystals, and the 40° peak indicates the presence of crystals. This result is consistent with the

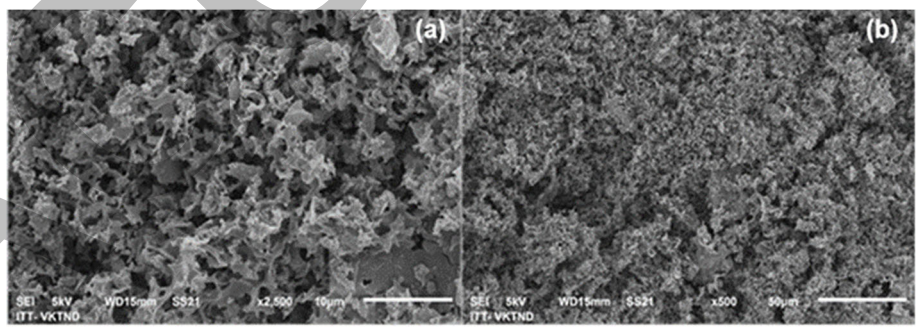

Fig 1. SEM images of activated carbon at (a) 10 μm and (b) 50 μm

Table 1. BET comparison of activated carbon materials from dragon fruit peels

STT	Materials synthesis method	Activation conditions	S_{BET} (m^2/g)	Ref.
1	Conventional method	700 °C – 60 min	756.300	[13]
2	Conventional method	800 °C – 120 min	1872.000	[16]
3	Microwave support method	600 W – 2 min	688.808	This study

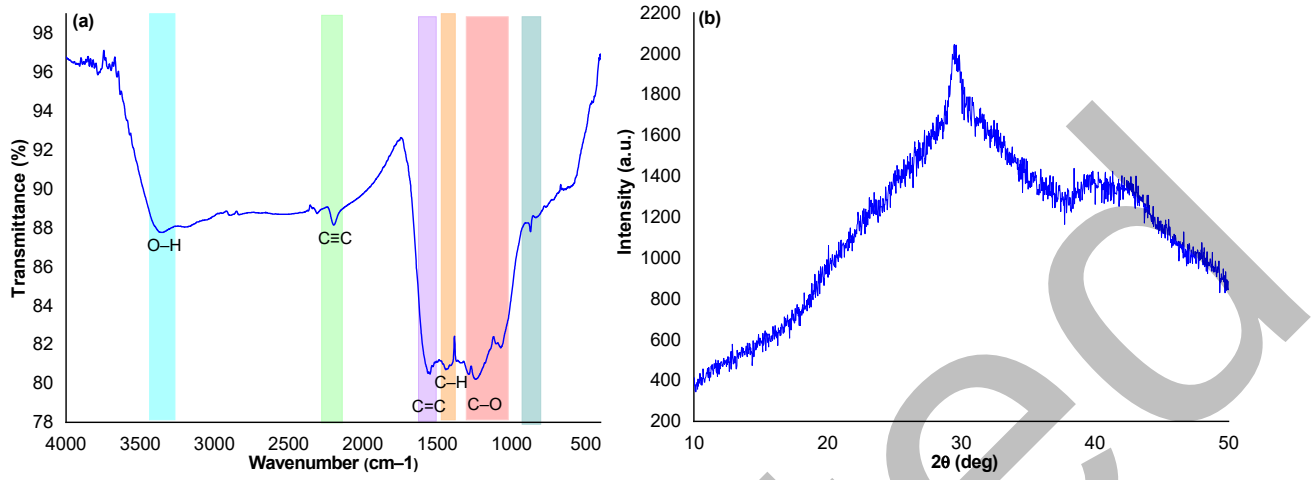

Fig 2. (a) FTIR and (b) XRD images of activated carbon from dragon fruit peel

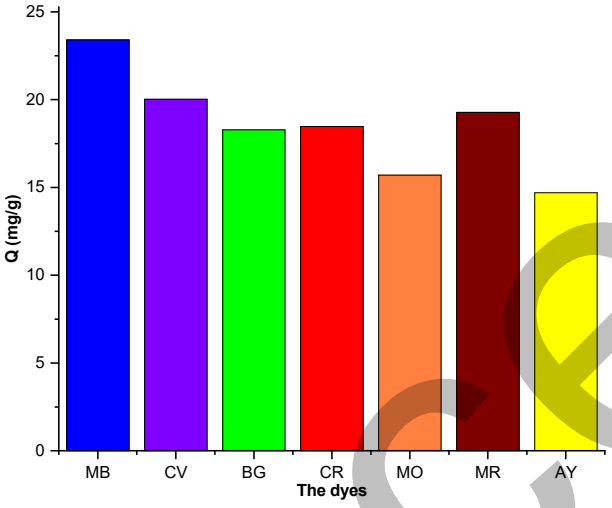

Fig 3. Selective adsorption capacity evaluation chart

study of Jawad et al. [13]. This shows that the material has great potential for application in adsorption research.

Evaluation of Selective Adsorption Capacity

Activated carbon is evaluated for its ability to selectively adsorb negative and positive organic pigments, with fixed factors, such as concentration, time 180 min, content 0.1 g/L, and temperature 30 °C. Fig. 3 shows that the adsorption capacity for gram-positive pigments, which are CV, BG, and MB, is quite high, with the adsorption capacity up to 16.47, 15.58, and 23.4 mg/g, respectively. Gram-negative pigments, MR and CR, have an adsorption capacity of 19.29 and 18.47 mg/g, respectively, and MO and AY are 15.7 and 14.6 mg/g, respectively. MB had the best adsorption capacity of 23.4 mg/g from all the colorants evaluated for selective adsorption. The FTIR results demonstrated that the material's surface, which is negatively charged due to the presence of hydroxyl groups, shows selective uptake for gram-positive dyes. This negative charge facilitates electrostatic interactions that enhance the selective adsorption of positively charged dyes. These findings suggest a promising approach for the filtration and separation of dye molecules. Given the results of the selective adsorption tests, MB was chosen for all subsequent evaluations. Therefore, MB will be used in the following experiments.

Evaluation of Factors Affecting the Adsorption Process

Effect of time and temperature on the adsorption process

Based on Fig. 4(a), the results of investigating the effect of time on the adsorption capacity are as follows. At the same concentration of 50 mg/L, at time points from 10 to 30 min, the adsorption capacity side effects tend to increase rapidly, the adsorption capacity increases from 42.993 to 47.703 mg/g. From 30–60 min, the adsorption capacity increased slightly to 48.805 mg/g. When up to 90 min, the adsorption capacity maintained a slight increase with the adsorption capacity of 49.715 mg/g. The adsorption capacity reached the maximum and remained stable at 120–180 min. The material's rapid initial adsorption rate for MB is likely attributed to the abundance of active sites on its surface. However, after 60 min, the substantial coverage of the

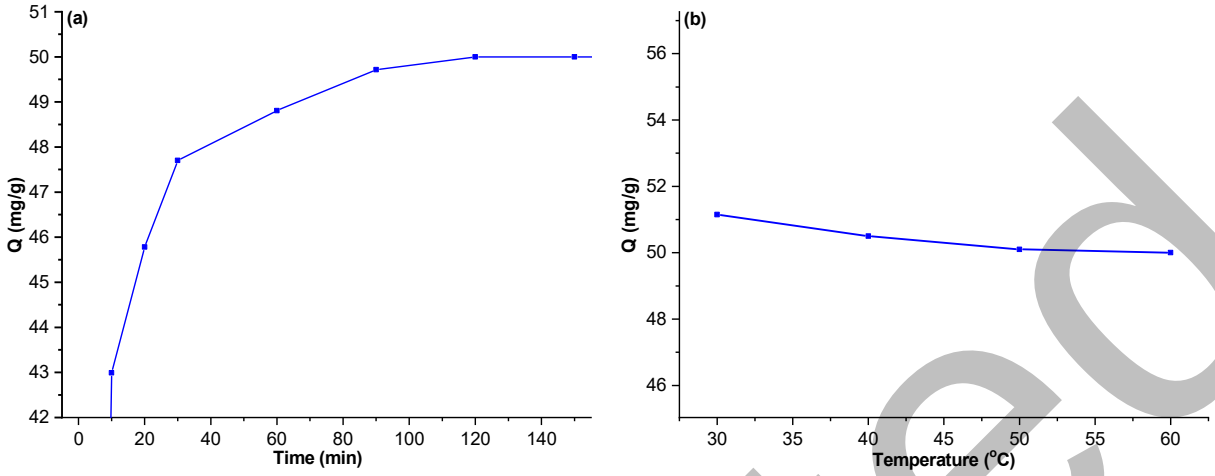

Fig 4. Adsorption capacity over (a) time and (b) temperature

surface by MB molecules may impede further adsorption, resulting in a slower rate [21]. Therefore, a 60 min period was selected for its high adsorption capacity, as the difference in adsorption at subsequent time points is minimal, thereby optimizing the process and saving time.

Based on Fig. 4(b), the results of investigating the influence of temperature on the adsorption capacity are as follows. With the same time and concentration, the adsorption capacity at the temperature milestones of 30, 40, 50, and 60 °C have adsorption capacity of 51.15, 50.50, 50.10, and 50.00 mg/g, respectively. The adsorption capacity tends to decrease with increasing temperature. That can be explained by the solubility of dyes increasing in solution, making them more difficult to adsorb on the surface of the material. According to Doumic et al. [22] at higher solution temperature, the electrostatic interaction becomes weaker, thus enhancing the desorption phenomenon. Similar results were also demonstrated by Djilani et al. [23]. Thus, the temperature level of 30 °C was selected to perform the following experiments.

Effect of pH

One critical parameter in adsorption studies is the solution pH, as it influences both the surface area of the adsorbent and the degree of ionization of MB molecules. Before assessing how pH affects the adsorption capacity of the material, the point of zero charge (pH_{pzc}) was determined to be 5.72. This indicates that at pH values below 5.72, the material's surface is positively charged, while at pH values above 5.72, the surface is negatively charged. The pH_{pzc} value can theoretically explain the influence of pH on the adsorption process based on electrostatic repulsion. The impact of pH on the adsorption capacity of MB was evaluated over a pH range of 2–10, with a fixed exposure time of 60 min, an adsorbent dose of 0.1 g, and an initial MB concentration of 50 mg/L, as shown in Fig. 5. As anticipated, electrostatic interactions between the positively charged MB cations and the negatively charged functional groups on the material enhanced the adsorption capacity. The maximum adsorption capacity of 46.67 mg/g for MB was achieved at pH 6. In acidic conditions, the low adsorption capacity is due to the excess H^+ ions competing with MB cations for active sites on the material's surface. Conversely, at higher pH levels, negatively charged OH^- ions on the adsorbent's surface increase, enhancing the electrostatic interactions with MB cations. Consequently, the highest removal efficiency of MB cations was observed at pH 6, which was selected for subsequent adsorption experiments.

Concentration and content

Fig. 6(a) illustrates how concentration affects the adsorption capacity of the material, with concentrations evaluated ranging from 0 to 200 mg/L. The adsorption capacity gradually increased from 0 to 40 mg/L. The adsorption capacity varied between 40 and 200 mg/L, peaking at 150 mg/L with a value of 60.26 mg/g. At low concentrations, the interaction between MB molecules and the adsorbent is strong due to the abundance of

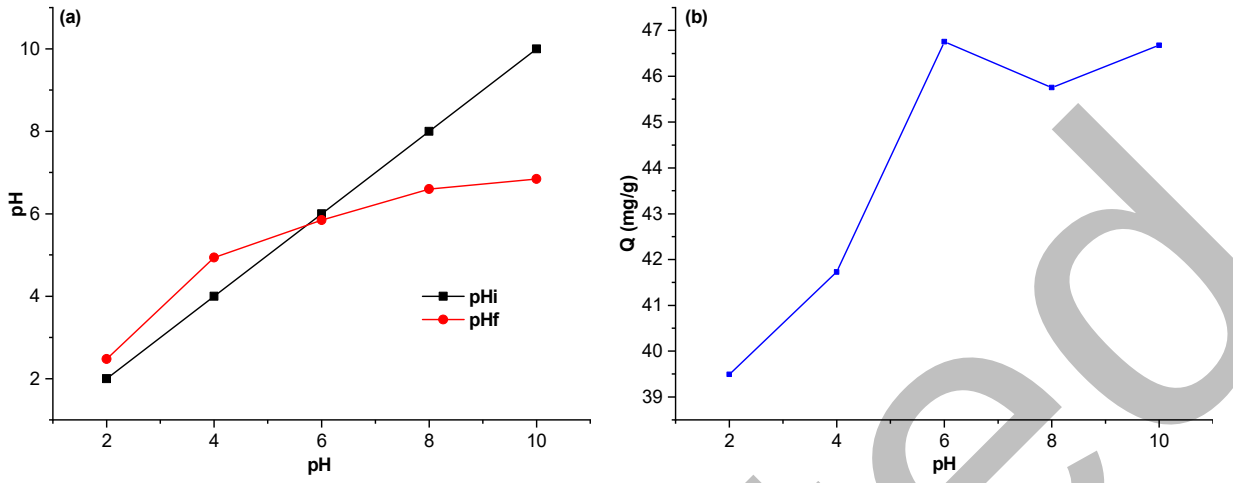

Fig 5. (a) The pH_{pzc} value of the material and (b) the adsorption capacity according to the solution pH

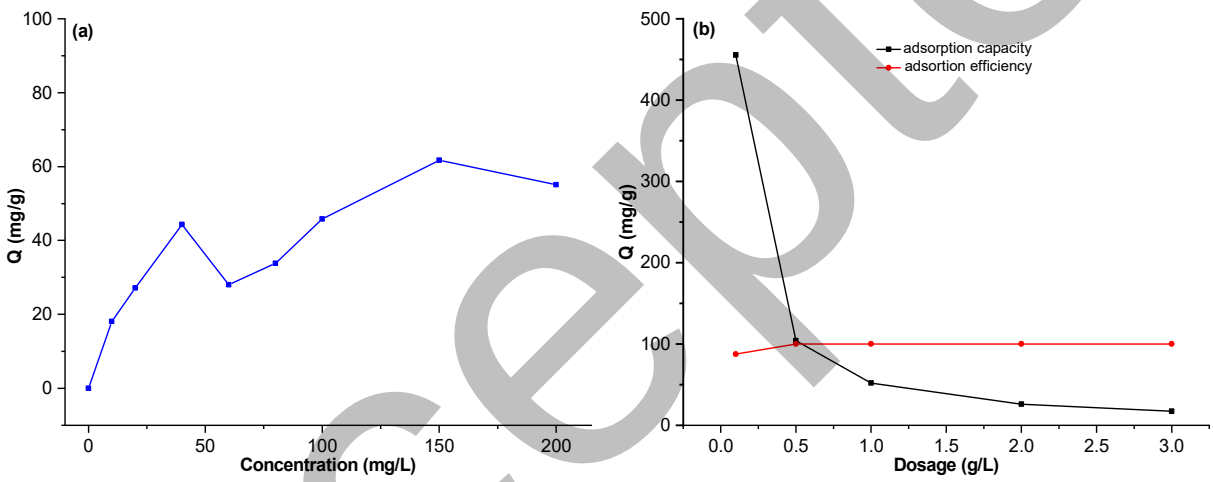

Fig 6. Adsorption capacity according to (a) dye concentration and (b) material content

vacant sites on the material's surface. However, as adsorption progresses, repulsive forces between the adsorbed MB molecules and those remaining in the solution develop, which impedes further adsorption.

Fig. 6(b) shows the influence of the content on the material's adsorption capacity. The assessed content values are 0.1, 0.5, 1.0, 2.0, and 3.0 g/L. As the material content increases, the adsorption capacity decreases because the adsorption capacity is evaluated based on the amount of color absorbed on the mass of the material. Therefore, the selection of the optimal concentration will also be based on the adsorption efficiency. At the concentration level of 0.1 g/L, the value reached 455.33 mg/g, 87.5%; concentration levels of 0.5, 1, 2, and 3 g/L, respectively, with adsorption capacity values of 104.08, 52.04, 26.02, and 17.35 mg/g and both have 100% adsorption efficiency. A concentration of 0.1 g/L was selected for the following experiments.

Evaluation of Kinetic Models

The adsorption kinetic model aims to elucidate the mechanisms underlying the adsorption process. Fig. 7 presents various kinetic models, including pseudo-first-order, pseudo-second-order, Elovich, and Bangham kinetics, along with the adsorption kinetics parameters for activated carbon derived from dragon fruit peel. These parameters are summarized in Table 2. The fit of the model is shown by the correlation coefficient (R^2), where the results are pseudo-first-order kinematics ($R^2 = 0.994$), pseudo-second-order kinematics ($R^2 = 0.999$), Elovich ($R^2 = 0.998$), and Bangham ($R^2 = 0.997$) models. Thus, the pseudo-second-order kinetic model is consistent

Table 2. Kinetic parameters for MB adsorption of activated carbon materials

Pseudo-first-order		Pseudo-second-order		Elovich		Bangham	
Qe (mg/g)	49.14	Qe (mg/g)	50.573	β (g/mg)	0.425	K_B	39.494
K_1	0.196	K_2	0.010	α (mg/g.min)	3.261	α	0.048
R^2	0.994	R^2	**0.999**	R^2	0.998	R^2	0.997

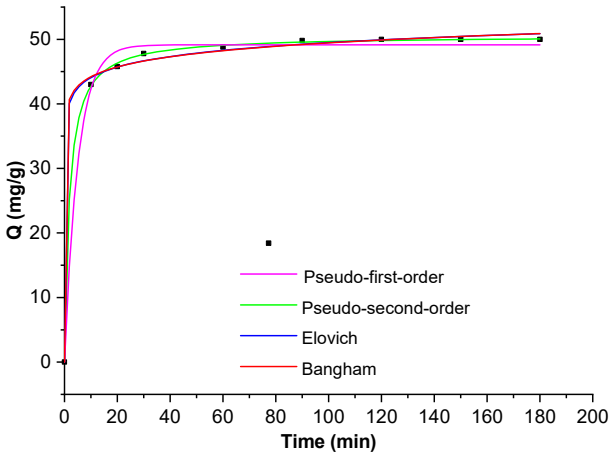

Fig 7. Adsorption kinetics model of activated carbon

with the adsorption data of activated carbon, which is demonstrated with the highest correlation coefficient. Ahmad et al. [14] also stated that activated carbon from the MB color-adsorbed dragon fruit peel is best suited to the pseudo-second-order kinetic model. The results show that the adsorption of activated carbon from dragon fruit peel is controlled mainly by chemisorption. This agreement is due to the interaction of the activated carbon through hydroxyl group with the N^+ moiety in the MB dye molecule.

Evaluation of Isotherm Models

The adsorption isotherm model is designed to characterize the adsorption process of different models. Fig. 8 illustrates the Langmuir, Freundlich, Temkin, and D-R isotherms, while Table 3 provides a summary of the corresponding isotherm parameters. The fit of the model is shown by the R^2. Temkin model has the highest correlation coefficient ($R^2 = 0.944$), Freundlich, Langmuir, D-R isotherm models have correlation coefficients of 0.943, 0.931, and 0.809, respectively. For the Langmuir model, an R_L value of 0.181 indicates that favorable adsorption is found in the range from 0 to 1. Thus, the Temkin and Freundlich adsorption isotherm models best fit the coal adsorption data. Activity from dragon fruit peel has been proven to have the highest correlation coefficient. The results show that the adsorption process is multilayer, heterogeneous, and diffuses on a uniform surface. This result is consistent with the previous studies [13,24].

Comparison with Other Studies

The adsorption capacity of activated carbon from NaOH-activated dragon fruit peel using the microwave-assisted method was compared with the adsorption

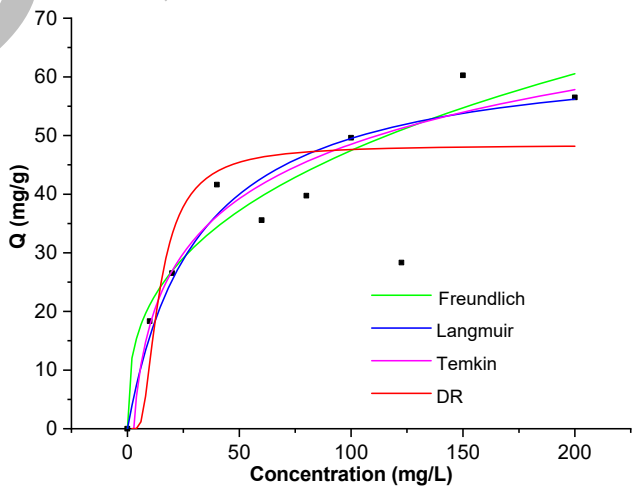

Fig 8. The adsorption isotherm model of activated carbon

Table 3. Isothermal parameters for MB adsorption of activated carbon

Freundlich		Langmuir		Temkin		D-R	
K_F (L/mg)	9.395	K_L (L/mg)	0.030	K_T	0.370	B (mol^2/kJ^2)	25.980
1/n	2.843	Q_m (mg/g)	65.010	B_T	13.421	Q_m (mg/g)	48.365
R^2	**0.943**	R^2	0.931	R^2	**0.944**	R^2	0.809
		R_L	0.181			E (kJ/mol)	0.139

Table 4. Comparison of MB pigment adsorption capacity of different activated carbon materials from previous studies

STT	Adsorbent materials	Synthetic process	Kinetic model	Isothermal model	Q_{max} (mg/g)	Ref.
1	Activated carbon from dragon fruit peel	Activation conditions: 700 °C, 60 min, N_2 gas (99.99%)	PFO	Langmuir	195.20	[13]
2	Activated carbon from acacia tree bark	Activation conditions: 1160 °C, Activator: NaOH	-	Langmuir	15.34	[25]
3	Activated carbon from wood	Activation conditions: 500 °C, 120 min, Activator: H_3PO_4	-	Langmuir	59.92	[26]
4	Activated carbon from watercress	Activation conditions: pure N_2 gas (99.99%), flow rate 150 mL/min	PSO	Freundlich	43.30	[24]
5	Activated carbon from bean shells	Activation conditions: 500 °C, 60 min, Activator: $ZnCl_2$	PSO	Langmuir	246.91	[27]
6	Activated carbon from tea residue	Activation conditions: gas N_2, 800 °C	PSO	Freundlich	238.10	[28]
7	Activated carbon from dragon fruit peel	Activation conditions: Microwave support 800 W, 2 min Activator: NaOH	PSO	Freundlich, Temkin	65.01	This study

capacity of other materials with different activation conditions, as summarized in Table 4. Activated carbon from dragon fruit peels is activated by NaOH using the microwave-assisted method with only a very low activation time, but the maximum adsorption capacity (Q_{max}) is quite relative compared to other research.

Optimization Using the RSM Model

The optimization of the MB adsorption process on activated carbon derived from dragon fruit peel was conducted using the response surface methodology (RSM) model. The influencing factors considered were solution pH, initial MB concentration, and adsorption time. These factors were evaluated at five levels: central (0), low (−1), high (+1), and ±α levels. Analysis of variance (ANOVA) was performed using Design-Expert software (version 11, State Ease, Minneapolis, USA). The ANOVA of the quadratic linear regression model was utilized to analyze the impact of input and output variables and the correlation between response functions and independent variables.

The RSM model was constructed incorporating central and boundary values using the optimal adsorption conditions. The experimental outcomes assessing the MB adsorption capacity of activated carbon materials are detailed in Tables 5 and 6. A total of 20 experiments were designed based on the RSM matrix. The RSM model generated residual value histograms, line plots, and 3D inter-factor charts alongside an analysis of the variance table. Evaluation outcomes from DX11 software for the quadratic regression equation delineate the relationship between the response value and independent variables, $Q\ (mg/g) = 59.918 - 0.04A - 2.258B - 4.643C + 4.027AB + 0.518AC - 1.11BC - 5.595A^2 - 13.029B^2 - 3.643C^2$.

Tables 7 and 8 present the ANOVA data for the regression equations. The significance of the regression models is assessed through the R^2, the p-value, and F-value. Generally, a smaller p-value and larger F-value indicate greater statistical significance of the model. A model is considered effective when $p < 0.05$, while it is deemed ineffective when $p > 0.05$. A p-value below 0.05 signifies the statistical significance of the influencing factors at a 95% confidence level. The ANOVA results indicate that the model exhibits statistical significance ($p < 0.05$), with a regression coefficient of $R^2 = 0.994 > 0.8$,

Table 5. Matrix of independent variables and levels

Independent factor	Level				
	−α	−1	0	1	+α
pH	2.64	4	6	8	9.36
Concentration (mg/L)	32.27	80	150	220	267.73
Time (min)	9.55	30	60	90	110.45

Table 6. Design table of 20 independent experiments

STT	pH	Concentration (mg/L)	Time (min)	Real value	Predicted value
1	6	150	9.54622	57.30	57.42
2	8	220	30	43.62	44.61
3	8	80	30	39.58	38.85
4	6	150	60	61.46	59.92
5	6	150	60	60.28	59.92
6	6	32.27450	60	26.37	26.86
7	9.36359	150	60	44.56	44.02
8	4	220	30	37.88	37.68
9	8	220	90	33.78	34.14
10	4	80	30	47.91	48.03
11	4	80	90	40.44	39.93
12	2.63641	150	60	44.30	44.16
13	6	150	60	61.64	59.92
14	6	150	60	59.55	59.92
15	4	220	90	23.93	25.13
16	6	150	110.45400	42.60	41.80
17	6	267.72500	60	20.44	19.27
18	6	150	60	58.82	59.92
19	6	150	60	57.64	59.92
20	8	80	90	32.15	32.83

indicating compatibility between the model and the experimental data. The factors with statistical significance ($p < 0.05$) are concentration and time, and the factor with no statistical significance is pH ($p > 0.05$). Parameters with p value > 0.05 will be excluded to fit the model best. This is also proved similarly in the study of Jawad et al. [13]. From practical experiments, surplus value charts have been obtained. The experiments are distributed independently of each other. From there, the RSM model was used to optimize the conditions in the experiment such as pH, color concentration (mg/L), and adsorption time. The optimal

Table 7. Analysis of variance mathematical model of activated carbon materials

Parameter	
SSres	18.43
SSlof	6.43
SSE	12.00
SStot	3296.82
MSE	2.40
R^2	0.9944
R^2 correction	0.9894
R^2 forecast	0.9790

Table 8. ANOVA values of the RSM model

Parameter	Sum of squares	Mean squared	F-value	P-value
Model	3278.38	364.26	197.60	< 0.0001
A-pH	0.0235	0.0235	0.0127	0.9124
B- Concentration	69.68	69.68	37.80	0.0001
C-Time	294.53	294.53	159.77	< 0.0001
AB	129.74	129.74	70.38	< 0.0001
AC	2.15	2.15	1.17	0.3051
BC	9.87	9.87	5.36	0.0432
A^2	451.14	451.14	244.73	< 0.0001
B^2	2446.65	2446.65	1327.21	< 0.0001
C^2	191.34	191.34	103.79	< 0.0001

value region of the model is shown in Fig. 9. The highest point of the model gives the optimal value of the material. The surface plots and 3D models show the evaluation model's optimal region. The interaction between the elements shows convergence in the 3D figure.

The optimal values will be determined and chosen according to the optimal region delineated by the influencing factors. As illustrated in Fig. 10, the optimal values for the material are distinctly indicated. Table 9 shows these optimal values were pH 6.25, concentration

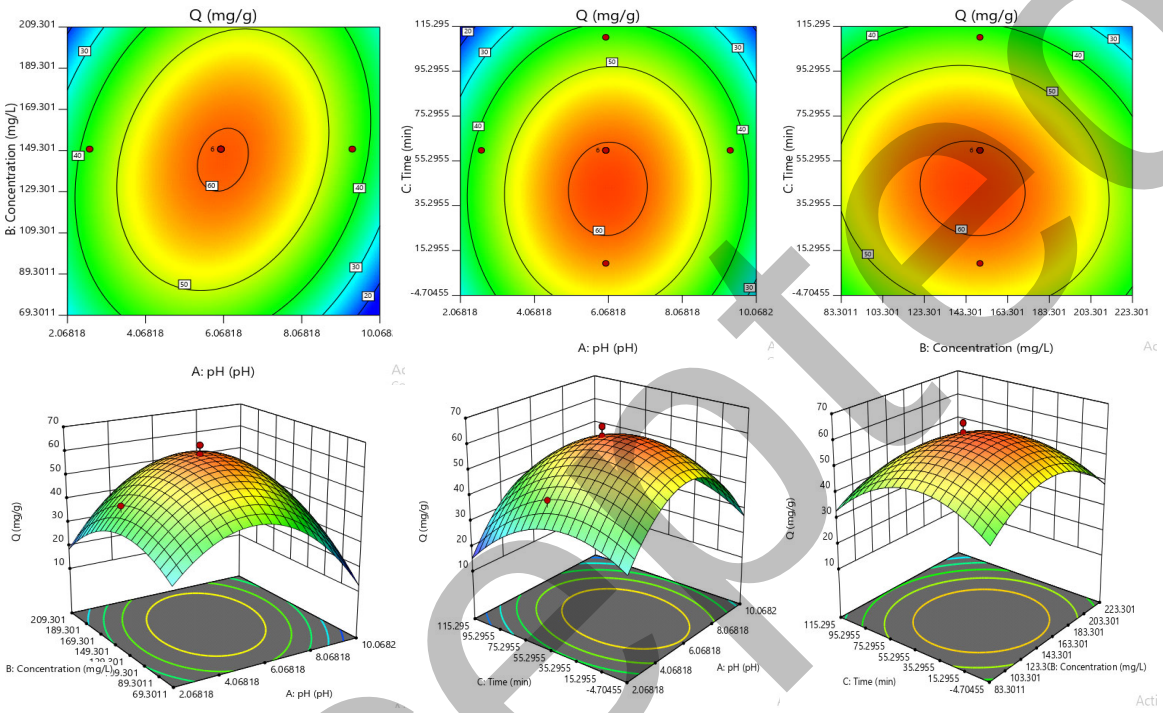

Fig 9. Line diagram and 3D histogram of materials

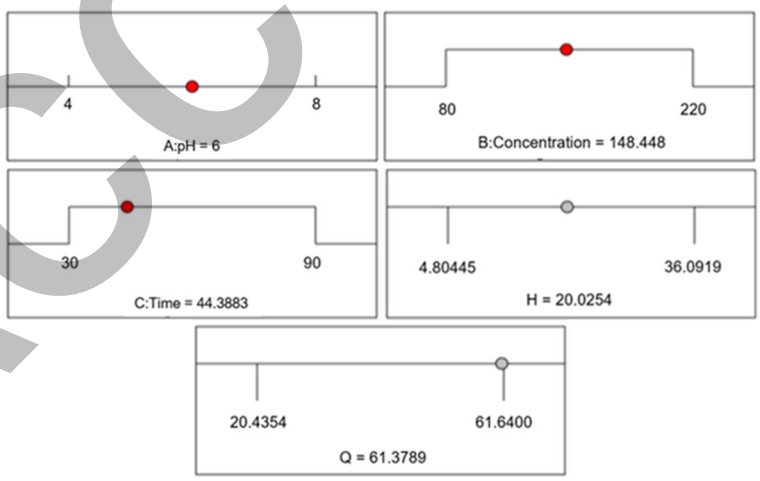

Fig 10. Optimal values from the model of materials

Table 9. Optimal model testing

Dyes	Concentration (mg/L)	pH	Time (min)	Adsorption capacity			Expected
				Forecast	Test	Error	
Methylene Blue	157.06	6.25	73.41	56.69	57.37	0.68	1

157.06 mg/L, and time 73.41 min. Under optimal conditions, the adsorption capacity predicted from the model is said to be 56.69 mg/g with an efficiency of 17.7%.

■ CONCLUSION

In this investigation, activated carbon derived from dragon fruit peel was synthesized and tested for its ability to adsorb organic pigments in aqueous solutions. The outcomes are that the synthesized activated carbon exhibited high efficacy in removing gram-positive MB dye from aqueous solutions. SEM and FTIR analyses confirmed the presence of characteristic functional groups indicative of activated carbon. The adsorption capacities for various dyes were assessed, with MB demonstrating the highest adsorption capacity. Results indicated minimal influence of content and temperature factors on adsorption, leading to the prioritization of pH, time, and color concentration for RSM model evaluation. From the RSM model, the factors have a clear interaction. The model's experiments are evenly distributed. The optimal points and regions are clearly shown. Since then, the optimal values have been recorded at pH 6.25, concentration 157.06 mg/L, time 73.41 min. Under optimal conditions, the adsorption capacity predicted from the model is said to be 56.69 mg/g with an efficiency of 17.7%. Besides, the PSO, Temkin, and Freundlich models are suitable for the adsorption kinetics and isotherms of the materials.

■ ACKNOWLEDGMENTS

This study was supported by grants from Nguyen Tat Thanh University, Ho Chi Minh City, Vietnam (SPUD.2024.01.05/HĐ-KHCN).

■ CONFLICT OF INTEREST

The authors have no conflict of interest.

■ AUTHOR CONTRIBUTIONS

Thi Ngoc Diem Tran conducted the experiment, Thi Tuu Tran, Ngoc Bich Hoang, and Van Tan Lam conducted the calculations, Thi Ngoc Diem Tran and Thi Cam Quyen Ngo wrote and revised the manuscript. All authors agreed to the final version of this manuscript.

■ REFERENCES

[1] Shao, Y., Wang, X., Kang, Y., Shu, Y., Sun, Q., and Li, L., 2014, Application of Mn/MCM-41 as an adsorbent to remove methyl blue from aqueous solution, *J. Colloid Interface Sci.*, 429, 25–33.

[2] Liu, Q., 2020, Pollution and treatment of dye waste-water, *IOP Conf. Ser.: Earth Environ. Sci.*, 514 (5), 052001.

[3] Samide, A., Tutunaru, B., Tigae, C., Efrem, R., Moanta, A., and Dragoi, M., 2014, Removal of methylene blue and methyl blue from wastewater by electrochemical degradation, *Environ. Prot. Eng.*, 40 (4), 93–104.

[4] Asghar, H.M.A., Ahmad, T., Hussain, S.N., and Sattar, H., 2015, Electrochemical oxidation of methylene blue in aqueous solution, *Int. J. Chem. Eng. Appl.*, 6 (5), 352–355.

[5] Rajoriya, S., Bargole, S., and Saharan, V.K., 2017, Degradation of a cationic dye (Rhodamine 6G) using hydrodynamic cavitation coupled with other oxidative agents: Reaction mechanism and pathway, *Ultrason. Sonochem.*, 34, 183–194.

[6] Nourmoradi, H., Zabihollahi, S., and Pourzamani, H.R., 2016, Removal of a common textile dye, navy blue (NB), from aqueous solutions by combined process of coagulation–flocculation followed by adsorption, *Desalin. Water Treat.*, 57 (11), 5200–5211.

[7] Bet-moushoul, E., Mansourpanah, Y., Farhadi, K., and Tabatabaei, M., 2016, TiO_2 nanocomposite based polymeric membranes: A review on performance improvement for various applications in chemical engineering processes, *Chem. Eng. J.*, 283, 29–46.

[8] Zhang, B., Wu, Y., and Cha, L., 2019, Removal of methyl orange dye using activated biochar derived from pomelo peel wastes: Performance, isotherm, and kinetic studies, *J. Dispersion Sci. Technol.*, 41 (1), 125–136.

[9] Juang, L.C., Wang, C.C., and Lee, C.K., 2006, Adsorption of basic dyes onto MCM-41, *Chemosphere*, 64 (11), 1920–1928.

[10] Danish, M., and Ahmad, T., 2018, A review on utilization of wood biomass as a sustainable precursor for activated carbon production and application, *Renewable Sustainable Energy Rev.*, 87, 1–21.

[11] Ahmad, M.A., Md Eusoff, M.A., Khan, M.N.N., and Khasri, A., 2019, Microwave-assisted activated carbon from passion fruit peel for methylene blue dye removal, *AIP Conf. Proc.*, 2124 (1), 030019.

[12] Lu, W., Cao, X., Hao, L., Zhou, Y., and Wang, Y., 2020, Activated carbon derived from pitaya peel for supercapacitor applications with high capacitance performance, *Mater. Lett.*, 264, 127339.

[13] Jawad, A.H., Saud Abdulhameed, A., Wilson, L.D., Syed-Hassan, S.S.A., ALOthman, Z.A., and Rizwan Khan, M., 2021, High surface area and mesoporous activated carbon from KOH-activated dragon fruit peels for methylene blue dye adsorption: Optimization and mechanism study, *Chin. J. Chem. Eng.*, 32, 281–290.

[14] Ahmad, M.A., Eusoff, M.A., Adegoke, K.A., and Bello, O.S., 2021, Sequestration of methylene blue dye from aqueous solution using microwave assisted dragon fruit peel as adsorbent, *Environ. Technol. Innovation*, 24, 101917.

[15] Georgin, J., da Boit Martinello, K., Franco, D.S.P., Netto, M.S., Piccilli, D.G.A., Yilmaz, M., Silva, L.F.O., and Dotto, G.L., 2022, Residual peel of pitaya fruit (*Hylocereus undatus*) as a precursor to obtaining an efficient carbon-based adsorbent for the removal of metanil yellow dye from water, *J. Environ. Chem. Eng.*, 10 (1), 107006.

[16] Neme, I., Gonfa, G., and Masi, C., 2022, Preparation and characterization of activated carbon from castor seed hull by chemical activation with H_3PO_4, *Results Mater.*, 15, 100304.

[17] Purnaningtyas, M.A.K., Sudiono, S., and Siswanta, D., 2020, Synthesis of activated carbon/chitosan/alginate beads powder as an adsorbent for methylene blue and methyl violet 2B dyes, *Indones. J. Chem.*, 20 (5), 1119–1130.

[18] Nayak, A., Bhushan, B., Gupta, V., and Kotnala, S., 2021, Fabrication of microwave assisted biogenic magnetite-biochar nanocomposite: A green adsorbent from jackfruit peel for removal and recovery of nutrients in water sample, *J. Ind. Eng. Chem.*, 100, 134–148.

[19] Bruice, P.Y., 2011, Beauchamp spectroscopy tables 1, *Org. Chem.*, 2620, A16–A17.

[20] Sigma-Aldrich, 2019, *IR spectrum table by frequency range*, https://www.sigmaaldrich.com/technical-documents/articles/biology/ir-spectrum-table.html, 1–6.

[21] Baheri, B., Ghahremani, R., Peydayesh, M., Shahverdi, M., and Mohammadi, T., 2016, Dye removal using 4A-zeolite/polyvinyl alcohol mixed matrix membrane adsorbents: Preparation, characterization, adsorption, kinetics, and thermodynamics, *Res. Chem. Intermed.*, 42 (6), 5309–5328.

[22] Doumic, L., Salierno, G., Cassanello, M., Haure, P., and Ayude, M., 2015, Efficient removal of Orange G using Prussian Blue nanoparticles supported over alumina, *Catal. Today*, 240, 67–72.

[23] Djilani, C., Zaghdoudi, R., Djazi, F., Bouchekima, B., Lallam, A., Modarressi, A., and Rogalski, M., 2015, Adsorption of dyes on activated carbon prepared from apricot stones and commercial activated carbon, *J. Taiwan Inst. Chem. Eng.*, 53, 112–121.

[24] Mousavi, S.A., Mehralian, M., Khashij, M., and Parvaneh, S., 2017, Methylene blue removal from aqueous solutions by activated carbon prepared from *N. microphyllum* (AC-NM): RSM analysis, isotherms and kinetic studies, *Global NEST J.*, 19 (4), 697–705.

[25] Nguyen, T.N., Dang, K.Q., and Nguyen, D.T., 2021, Adsorptive removal of methyl orange and methylene blue from aqueous solutions with *Acacia crassicarpa* activated carbon, *Vietnam J. Sci., Technol. Eng.*, 63 (4), 23–27.

[26] Danish, M., Ahmad, T., Hashim, R., Said, N., Akhtar, M.N., Mohamad-Saleh, J., and Sulaiman, O., 2018, Comparison of surface properties of wood biomass activated carbons and their application against rhodamine B and methylene blue dye, *Surf. Interfaces*, 11, 1–13.

[27] Geçgel, Ü., Özcan, G., and Gürpınar, G.Ç., 2013, Removal of methylene blue from aqueous solution by activated carbon prepared from pea shells (*Pisum sativum*), *J. Chem.*, 2013 (1), 614083.

[28] Tuli, F.J., Hossain, A., Kibria, A.K.M.F., Tareq, A.R.M., Mamun, S.M.M.A., and Ullah, A.K.M.A., 2020, Removal of methylene blue from water by low-cost activated carbon prepared from tea waste: A study of adsorption isotherm and kinetics, *Environ. Nanotechnol., Monit. Manage.*, 14, 100354.